

Time resolved magneto-optical spectroscopy on InGaAs nanostructures grown on (311)A and (100)-oriented substrates

M. Lomascolo, R. Cingolani, P. O. Vaccaro, and K. Fujita

Citation: [Applied Physics Letters](#) **74**, 676 (1999); doi: 10.1063/1.122984

View online: <http://dx.doi.org/10.1063/1.122984>

View Table of Contents: <http://scitation.aip.org/content/aip/journal/apl/74/5?ver=pdfcov>

Published by the [AIP Publishing](#)

Articles you may be interested in

[Single quantum dot emission at telecom wavelengths from metamorphic InAs/InGaAs nanostructures grown on GaAs substrates](#)

Appl. Phys. Lett. **98**, 173112 (2011); 10.1063/1.3584132

[Temperature dependence of time-resolved photoluminescence spectroscopy in InAs/GaAs quantum ring](#)

Appl. Phys. Lett. **94**, 183101 (2009); 10.1063/1.3130741

[Time-resolved photoluminescence spectroscopy of subwetting layer states in In Ga As/Ga As quantum dot structures](#)

J. Appl. Phys. **100**, 054316 (2006); 10.1063/1.2345464

[Exciton localization in In 0.15 Ga 0.85 As/GaAs quantum wire structures grown on \(553\)B-oriented GaAs substrate](#)

J. Appl. Phys. **90**, 5111 (2001); 10.1063/1.1412271

[InGaAs/GaAs quantum nanostructure fabrication on GaAs \(111\)A vicinal substrates by atomic layer epitaxy](#)

J. Appl. Phys. **83**, 5525 (1998); 10.1063/1.367406

An advertisement for Keysight B2980A Series Picoammeters/Electrometers. The ad features a red and white color scheme. On the left, there is a red button with the text 'View video demo'. In the center, there is a photograph of the Keysight B2980A device. On the right, there is the Keysight Technologies logo, which consists of a red stylized 'K' followed by the text 'KEYSIGHT TECHNOLOGIES'. The main text of the ad reads: 'Confidently measure down to 0.01 fA and up to 10 PΩ' and 'Keysight B2980A Series Picoammeters/Electrometers'.

Time resolved magneto-optical spectroscopy on InGaAs nanostructures grown on (311)A and (100)-oriented substrates

M. Lomascolo^{a)} and R. Cingolani

Istituto Nazionale per la Fisica della Materia, Unità di Lecce, Dipartimento di Scienza dei Materiali, Università di Lecce, via per Arnesano, I-73100 Lecce, Italy

P. O. Vaccaro and K. Fujita

ATR Adaptive Communications Research Laboratories, 2-2 Hikaridai Seika-cho, Soraku-gun, Kyoto 619-02, Japan

(Received 11 September 1998; accepted for publication 18 November 1998)

We present a time-resolved magneto-photoluminescence study of $\text{In}_{0.5}\text{Ga}_{0.5}\text{As}$ self-organized nanostructures grown on (100) and (311)A-oriented substrates by molecular beam epitaxy. The (311)A-oriented samples have a corrugated surface realizing a sort of quantum wire array, whereas the (100) samples exhibit Stranski–Krastanow islands. The different morphology of the nanostructures is reflected in the different electron/hole wave-function confinement along the three directions (perpendicular and parallel to the growth direction). We discuss the effects of the magnetic field (up to 8 T) on the recombination mechanism in these InGaAs nanostructures and on the transient dynamics of photoluminescence. We observe a clear decrease of the photoluminescence decay time with magnetic field flux indicating the exciton nature of the radiative low-temperature recombination processes. © 1999 American Institute of Physics. [S0003-6951(99)04004-8]

The application of an external perturbation such as a magnetic field, introduces strong modifications of the density of states of nanostructures.¹ By increasing the magnetic field strength, it is possible to investigate different exciton confinement regimes, from the low field limit in which the magnetic field is a minor perturbation with respect the Coulomb interaction (diamagnetic shift), to the high field limit in which the magnetic field influences the electron and hole motion (cyclotron motion) stronger than the Coulomb interaction (Landau shift).^{2,3} This condition is particularly interesting in three dimensionally confined nanostructures in which the discrete density of states imposes severe constraints to the thermalization processes of excitons and carriers.

In this letter, we discuss the effects of the magnetic field on the recombination dynamics of excitons in highly strained wire-like and dot-like $\text{In}_{0.5}\text{Ga}_{0.5}\text{As}$ nanostructures.

Two different nanostructure systems were grown by molecular beam epitaxy (MBE) on semi-insulating (311)A and (100)-GaAs oriented substrates, both consisting of 6 monolayers of $\text{In}_{0.5}\text{Ga}_{0.5}\text{As}$. The (311)A-oriented samples have a corrugated surface realizing a quantum wire array of periodicity 35 nm and height 2 nm. The 6 monolayer (ML) (100) sample presents the usual Stranski–Krastanow growth mode with islands of diameter 25 nm and height of 3 nm. The full optical and structural characterization of the samples has been reported in Refs. 4 and 5. Continuous wave photoluminescence (PL) was excited by the 514.5 nm line of a Ar⁺ laser and dispersed by a 1 m single monochromator equipped with a cooled Ge detector. The excitation power was varied from a few mW to hundreds mW in order to saturate localization. Transient photoluminescence (TPL) was excited by a 2 ps pulsed Ti:Sapphire laser operating at 82 MHz repetition

rate, and analyzed by a synchroscan streak camera equipped with a two dimensional cooled charge coupled device. The overall time resolution is about 15 ps. The samples were mounted in a superconducting magnet in which the magnetic field orientation could be changed from parallel to perpendicular to the growth direction.

The different morphology of the nanostructures affects the electron/hole wave-function confinement along the three different directions (perpendicular versus parallel to growth direction). If the magnetic length $l = \sqrt{\hbar/eB}$ is larger than the transverse extension of the exciton wave-function $\xi = \sqrt{\langle \Psi | x^2 + y^2 | \Psi \rangle}$ (which is related to the quasi-two-dimensional Bohr radius), the interaction of the exciton with the magnetic field (B) manifests itself by a diamagnetic shift quadratic in B :³

$$\Delta E_{\text{exc}} = \frac{e^2 B^2}{8\mu} \langle \Psi | x^2 + y^2 | \Psi \rangle,$$

where μ is the reduced mass and $|\Psi\rangle$ the exciton wave-function. If the strength of the magnetic field is large enough to make $1 \leq \xi$, than a more pronounced energy shift, either quadratic or linear in B depending on the potential symmetry,⁶ occurs (free carrier case).

Due to the morphology of our samples, when the magnetic field is perpendicular to the growth direction, we probe the lateral extension of the wave-function along the less confined direction. In this case, a small parabolic-like diamagnetic shift of about 3 meV of the PL is observed (up to 8 T) in both the 0D and 1D nanostructures, as reported in Fig. 1. In Fig. 2, we show the energy of the PL peaks vs B (open circles refer to (100)-oriented samples, full circles refer to (311)A-oriented samples).

By using a linear interpolation of the GaAs and InAs masses and dielectric constants,^{7,8} we fit the expression of the diamagnetic shift to the experimental data, by using the transverse extent of the wave-function as the only adjustable

^{a)}Electronic mail: lomascolo@axpmat.unile.it

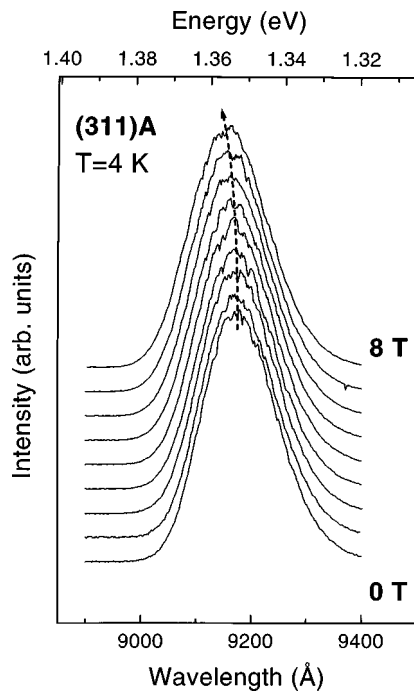


FIG. 1. Low temperature PL for the (311)A wire-like sample, recorded with increasing magnetic field.

parameter (Fig. 2, continuous and dotted lines). In both cases, the best fit value of the exciton extension results to be around 6 nm indicating the strong exciton confinement in both structures. A much larger shift is indeed obtained if we assume the bulk Bohr radius of 18.3 nm (see Fig. 2).

For the corrugated surface sample (311)A, the lateral extension of the wire is estimated to be less than 10 nm.^{4,5} The (100)-oriented sample with 6 ML of InGaAs presents islands with a diameter of 25 nm. In both cases, the exciton lateral dimension in the nanostructures is well below the magnetic length (about 10 nm at 8 T), suggesting an electron-hole recombination mechanisms in such nanostructures.

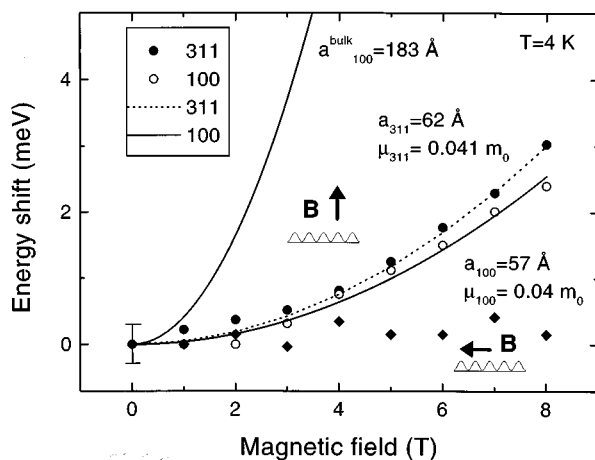


FIG. 2. Experimental (symbols) and calculated (lines) diamagnetic shift for the (100-empty symbols) and (311-full symbols) samples. The circles refer to the experiments with the magnetic field aligned parallel to the growth direction, whereas the diamonds refer to the experiments performed on the (311)A samples with the magnetic field aligned perpendicular to the growth direction and to the wire direction. The error bar represents the energy resolution of the experimental set-up.

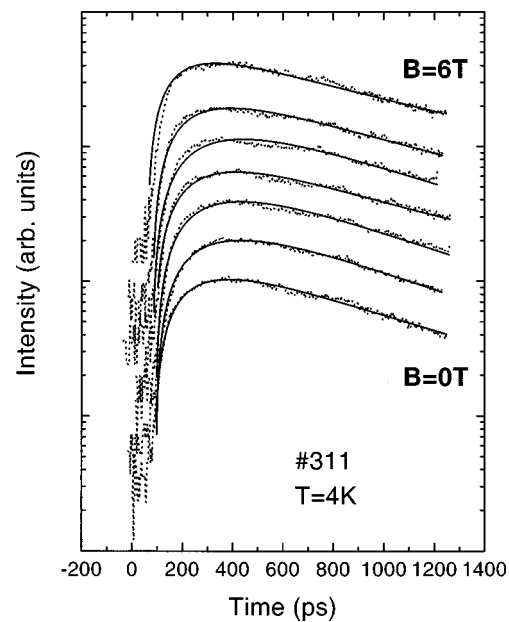


FIG. 3. Time evolution of the PL resonance for the (311)A wire-like samples at different magnetic field (dotted lines). Continuous lines through the experimental traces have been obtained by fitting the traces to a three-level model.

Furthermore, in the case of the (311)A-oriented samples, we performed an additional experiment with the magnetic field perpendicular to the growth direction and to the wire direction. Under this condition, the carriers motion probes the more confined direction, which is geometrically delimited by the height of the wires (about 2 nm). In this case, no PL energy shift is observed with increasing magnetic field up to 8 T (full diamond in Fig. 2), consistent with the very strong confinement of the exciton wave-function expected in this direction.

The exciton dynamics of these nanostructures displays important changes in magnetic field. This is investigated by time resolved photoluminescence at low temperature, setting the field direction parallel to the growth axis, and the excitation power density above about 20 kW/cm⁻², to get rid of localization. Normalized low temperature TPL traces for the (311)A-oriented sample as a function of the magnetic field are shown by the dotted lines in Fig. 3 [similar results are obtained for the (100) samples]. All the traces exhibit a luminescence rise time of about 200 ps and a mono exponential decay.

The time constants were obtained by fitting the traces to a three-level model⁹ given by

$$I(t) \propto \frac{\tau_r}{\tau_r - \tau_d} (e^{-t/\tau_d} - e^{-t/\tau_r}).$$

The time constant τ_r (PL rise time) and τ_d (PL decay time) are plotted in Figs. 4(a) and 4(b) as a function of the magnetic field strength [full circles refer to (311)A-oriented samples, open circles refer to (100)-oriented samples].

The rise time for the two different nanostructures is almost constant over the whole range of magnetic strength and it is equal to about 150–200 ps. This suggests that in the range 0–8 T, the carrier relaxation and diffusion from the barrier into the nanostructure are not drastically affected by the magnetic field. On the other hand, the decay time slightly

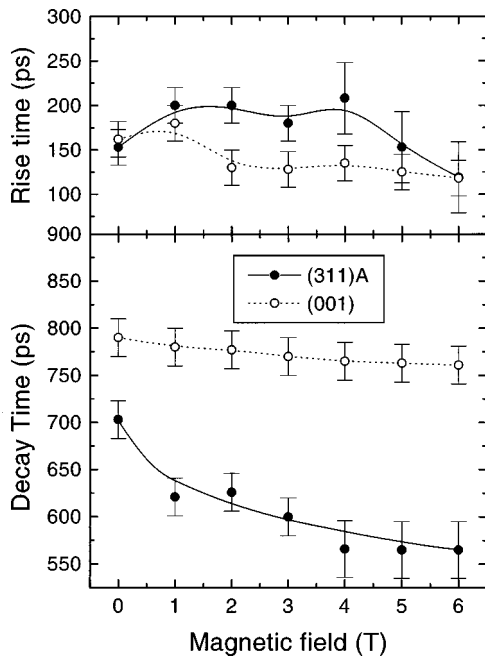


FIG. 4. Rise and decay time constants, obtained by fitting the traces to a three-level model, as a function of magnetic field. Lines through the data are a guide for the eyes.

decreases from about 800 to 760 ps, with increasing magnetic strength in the (100)A-oriented samples and in a more pronounced way in the quantum wire-like (311) samples, from 700 to 530 ps. This is consistent with the enhanced overlap of the electron/hole wave-function induced by the magnetic field which squeezes the exciton wave-function in the nanostructure.

It is known that the exciton radiative life-time reflects the dimensionality of the semiconductor heterostructure, and for 2D, 1D, and 0D it reads:^{10–13}

$$\tau_d^{2D} = \frac{\xi}{fA_c},$$

$$\tau_d^{1D} \propto \frac{1}{f} \sqrt{\frac{Mk_B T}{\hbar^2 k_{ex}^2}},$$

$$\tau_d^{0D} \propto \frac{1}{P^2} \frac{1}{|\int \phi_{ex}(r,r) dr|^2},$$

where A_c is the exciton coherence area, and f is the exciton oscillator strength;^{10,11} k_{ex} is the maximum radiative exciton wave number, T is the lattice temperature, and M is the total exciton mass. The oscillator strength f is proportional to the overlap of the electron and hole wave-functions and to the dipole matrix element P between the e/h states and the crystal ground state. $\phi(r,r)$ is the exciton envelope wave-function.

The effect of the magnetic field is to squeeze the exciton wave-function around the direction of the magnetic field, resulting in three main effects: (i) a decrease of the lateral extension ξ of the exciton wave-function; (ii) an increase of the coherence area (2D case), which is proportional to the exciton dephasing time; and (iii) an increase of the oscillator strength (2D and 1D), due to the larger probability to find the electron-hole pair closer in the same area. These effects

macroscopically manifest themselves by the reduction of the exciton decay-time in Fig. 4 for the wire-like (311)A sample.

On the other hand, in the 0D systems, if the magnetic length is larger than the Bohr radius, as in our experiments, the integral of the exciton wave-function is not expected to vary appreciably. The dependence on magnetic field is indeed contained in the oscillator strength (linearly related to the dipole matrix element). This is clearly seen in the little change of decay time occurring in the dot-like (100) samples in Fig. 4.

In all cases, the overall result is a decrease of the exciton radiative life-time with increasing magnetic field, as observed in our experiments.

Furthermore the (311)A wires-like samples present a shorter exciton life-time compared to the (100) dots-like one. Despite the larger oscillator strength expected in 0D confined samples, the relaxation processes in the dots could be slower.^{16–18} Moreover the (311)A wire-like sample has been found to be more affected by localization at interface monolayer fluctuation, as revealed by the constant decay time up to 100 K in the experiments reported in Ref. 4.

In conclusion, we have discussed the effects of the magnetic field (up to 8 T) on the recombination mechanism in $\text{In}_{0.5}\text{Ga}_{0.5}\text{As}$ nanostructures. The reduction of the PL decay time with increasing the magnetic field has been observed by time resolved magneto photoluminescence up to 6 T. This is related to the squeezing of the exciton wave-function around the direction of the magnetic field.

This work has been supported by the ‘‘Project 40% MURST-Physics of nanostructures,’’ and by EL-TMR Network ‘‘Ultrafast Quantum Optoelectronics.’’ The technical help of D. Cannoletta and A. Melcarne is gratefully acknowledged.

¹S. Raymond, S. Fafard, P. J. Poole, A. Wojs, P. Hawrylak, S. Charbonneau, D. Leonard, R. Leon, P. M. Petroff, and J. L. Merz, *Phys. Rev. B* **54**, 11548 (1996).

²M. Sugawara, N. Okazaki, T. Fujii, and S. Yamazaki, *Phys. Rev. B* **48**, 8848 (1993).

³P. V. Giugno, A. L. Convertino, R. Rinaldi, R. Cingolani, J. Massies, and M. Leroux, *Phys. Rev. B* **52**, 11591 (1995).

⁴P. O. Vaccaro, K. Fujita, and T. Watanabe, *Jpn. J. Appl. Phys., Part 1* **36**, 1948 (1997).

⁵P. O. Vaccaro, M. Hirai, K. Fujita, and T. Watanabe, *J. Phys. D* **29**, 2221 (1996).

⁶R. Rinaldi, P. V. Giugno, R. Cingolani, F. Rossi, E. Molinari, U. Marti, and F. K. Reinhart, *Phys. Rev. B* **53**, 13710 (1996).

⁷P. O. Vaccaro, K. Tominaga, M. Hosoda, K. Fujita, and T. Watanabe, *Jpn. J. Appl. Phys., Part 1* **34**, 1362 (1995).

⁸P. O. Vaccaro, M. Takahashi, K. Fujita, and T. Watanabe, *Jpn. J. Appl. Phys., Part 2* **34**, L13 (1995).

⁹G. Bastard, *Wave Mechanics Applied to Semiconductor Heterostructures* (Les Ulis, France, 1988).

¹⁰J. Feldman, G. Peter, E. O. Gobel, P. Dawson, K. Moore, C. Foxon, and R. Elliott, *Phys. Rev. Lett.* **59**, 2337 (1987).

¹¹D. S. Citrin, *Phys. Rev. Lett.* **69**, 3393 (1992).

¹²L. C. Andreani, in *Confined Electron and Photons*, NATO ASI Series Vol. B340, Edited by E. Burstein and C. Weisbuch (1995), p. 101.

¹³U. Bockelmann, *Phys. Rev. B* **48**, 17637 (1993).

¹⁴I. Aksenov, J. Kusano, Y. Aoyagi, T. Sugano, T. Yasuda, and Y. Segawa, *Phys. Rev. B* **51**, 4278 (1995).

¹⁵I. Aksenov, Y. Aoyagi, J. Kusano, T. Sugano, T. Yasuda, and Y. Segawa, *Phys. Rev. B* **52**, 17430 (1995).

¹⁶U. Bockelmann and G. Bastard, *Phys. Rev. B* **42**, 8947 (1990).

¹⁷H. Benisty, C. M. Sotomayor Torres, and C. Weisbuch, *Phys. Rev. B* **44**, 10945 (1991).

¹⁸T. Inoshita and H. Sakaki, *Phys. Rev. B* **46**, 7260 (1992).